Passive Method for Estimating Fundamental Frequency Grid Impedance: Including Model and Field Verification

Guerreiro, Gabriel Miguel Gomes; Sharma, Ranjan; Martin, Frank; Goldenbaum, Nikolaus; Yang, Guangya

Published in:
IEEE Transactions on Sustainable Energy

Link to article, DOI:
10.1109/TSTE.2025.3545342

Publication date:
2025

Document Version
Peer reviewed version

Passive Method for Estimating Fundamental Frequency Grid Impedance: Including Model and Field Verification

Gabriel Miguel Gomes Guerreiro, *Member, IEEE,* Ranjan Sharma, Frank Martin, Nikolaus Goldenbaum, Guangya Yang, *Senior Member, IEEE,*

***Abstract*—This letter presents a field-verified passive method to estimate the equivalent fundamental frequency grid impedance. The method requires reactive power, active power, and root-mean-square voltage measurements as inputs and is based on a mathematical derivation independent of the angle and frequency estimation. A thorough verification process was adopted, comprising simulations in EMT utilizing a wind turbine with actual control code, field wind turbine measurements, and an operational wind power plant where the transmission system operator agreed to change grid configurations to allow testing of the algorithm for two grid scenarios. Results show good agreement between expectations and estimation from the proposed method.**

***Index Terms*—Grid Impedance, Estimation, Passive Method, Field Verification.**

I. Introduction

THE rise of large-scale wind power plants (WPPs) and inverter-based resources (IBRs) will significantly complicate power system design and operation. Understanding the grid and its conditions is essential during both the design phase and the operational lifetime of the WPP [1]. Grid impedance can change over time [2], affecting grid compliance and stability. Most current studies on the impact of grid impedance on wind power performance rely on offline worst-case scenarios. This approach often results in inefficient site capacity utilization, suboptimal controller performance, and oversized reactive compensation equipment. Consequently, estimating grid impedance can benefit plant owners and system operators.

Methods for estimating grid impedance are mainly divided into two categories: active/invasive and passive/non-invasive methods [3]. Active methods rely on the injection of signals or manipulation of existing fundamental or harmonic components for estimating the grid impedance [4]. These methods tend to be more accurate than passive methods, but the major drawback is that they can introduce new disturbances in the power system. Passive methods rely on the measurements available without any additional disturbance introduced and can be divided into three approaches: Local PMU observers, PCC observers, and Kalman filters. The first two methods generally rely on local measurements that either capture data between two points in the network or at two distinct time instances, using algebraic equations to estimate impedance based on these measurements. However, these estimations are often hindered by frequency estimation reliance and measurement noise, making accurate results difficult to obtain [3]. In many cases, these methods require significant network variations (typically 3% or more) over consecutive measurements to reliably estimate the grid impedance [5]. Additionally, Kalman filters, which have gained popularity in controlled lab environments, are particularly sensitive to the quality of the initial system model and the covariance matrices, requiring careful parameter tuning [6]. This can be particularly challenging in real-world applications, where the true system parameters are often unknown or based on approximations. As such, the transition from simulation to testing in actual turbines or operational wind power plants can pose significant difficulties.

A passive estimation method (patent-pending [7]) is presented in this letter. The key advantages of the proposed method are its independence from large system variations, prolonged measurement periods, or data from multiple network locations. Additionally, it avoids the need for extensive hyperparameter tuning of optimization algorithms, as the same tolerance levels are used across all setups, simplifying its implementation and improving its applicability in dynamic and real-world environments. The method has proven to be more robust to noise, accurate, and fast for real-life applications. The method is also verified against field wind turbine generators (WTGs) and WPPs, and to the authors' knowledge, this is the first method tested extensively in such scenarios. The estimation method can be used for design, planning, and even real-time control optimization of different types of plants. The summarized contributions of this letter are:

1) Proposal of a novel method for estimation of equivalent grid impedance.
2) Verification against simulations and field measurements.

II. Methodology

This section presents the mathematical formulation and a description of the optimization-based estimation methods.

A. Mathematical Formulation

In Fig. (1), a generation bus is connected to the grid where current I_{bus} is measured and the angle δ_{ibus} is relative to voltage V_{bus}. The bus can be either at the unit- or at the plant-

Gabriel M.G. Guerreiro, Ranjan Sharma, and Nikolaus Goldenbaum are with Siemens Gamesa Renewable Energy A/S, 7330 Brande, DK, e-mail: gabriel.gomes@siemensgamesa.com.

Gabriel M.G. Guerreiro and Guangya Yang are the Department of Wind & Energy Systems, Technical University of Denmark, 2800 Kgs Lyngby, DK

Frank Martin is with European Energy A/S, Søborg, DK

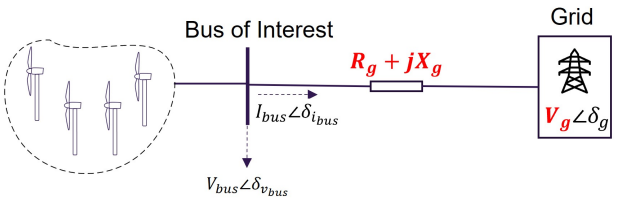

Fig. 1. Single line diagram of the system evaluated.

level. A grid equivalent is represented by a resistance (R_g) and a reactance (X_g), and a voltage source of magnitude (V_g) and angle (δ_g). Consider (1), where all values are represented in the complex plane. To find $\overline{Z}_g$, the angle different between $\overline{V}_{bus}$ and $\overline{V}_g$ needs to be known. Measuring reliable voltage angle and angle difference is complex. Therefore, this formulation removes this dependency.

$$\overline{V}_{bus} = \overline{I}_{bus} \cdot \overline{Z}_g + \overline{V}_g \tag{1}$$

If the current at the bus $\overline{I}_{bus} = \left(\frac{\overline{S}_{bus}}{\overline{V}_{bus}}\right)^*$ is considered and further substituted in (1), yielding (2):

$$\overline{V}_g = \overline{V}_{bus} - \left(\frac{\overline{S}_{bus}}{\overline{V}_{bus}}\right)^* \cdot \overline{Z}_g \tag{2}$$

Multiplying the two sides of (2) by its conjugates, (3) is obtained:

$$V_g^2 = V_{bus}^2 + \left(\frac{S_{bus}}{V_{bus}}\right)^2 \cdot Z_g^2 - 2Re\left(\left(\frac{\overline{S}_{bus}}{\overline{V}_{bus}}\right) \cdot \overline{Z}_g^* \cdot \overline{V}_{bus}\right) \tag{3}$$

Knowing that $\overline{Z}_g = R_g + jX_g$ and $\overline{S}_{bus} = P_{bus} + jQ_{bus}$, equation (3) can be further developed in (4):

$$V_g^2 = V_{bus}^2 + \left(\frac{S_{bus}}{V_{bus}}\right)^2 \cdot Z_g^2 - 2\left(R_g \cdot P_{bus} + X_g \cdot Q_{bus}\right) \tag{4}$$

Equation (4) does not contain any complex terms. The dependency on the angle difference between the bus of interest and the infinite bus has been eliminated. The equation has three unknowns (i.e., V_g, R_g and X_g) and three known variables that correspond to the measurements at the desired generation bus (i.e., P_{bus}, Q_{bus} and V_{bus}).

B. Optimization Problem

Equation (4) is utilized for the optimization problem and formulated as a quadratic error between the left and right side of the equation. Two optimization algorithms are selected due to their speed and accuracy when handling non-convex-constrained problems, namely Sequential Constrained Least-Squares Method (SLSQP) and Constrained Optimization BY Linear Approximations (COBYLA) [8], [9]. Random values of V_g, R_g and X_g are used to initialize algorithms at t = 0, and from then an average of the past five estimations are used to initialize. At each estimation step, five samples of P_{bus}, Q_{bus} and V_{bus} are used to make the estimation more robust to noise; therefore, a single value for the three unknowns must be found for the five different measurement points utilized.

The SCR is the measure of the grid strength, and there are several ways to define it. For the sake of this letter, SCR is expressed in p.u. with respect to the bus of interest. Equation (5) showcases the steps to obtain the simplified final version. Initially, the ratio between short-circuit power from the grid S_{SC} and the rated power of the bus of interest is defined. By applying modifications and multiplying both the numerator and denominator by the base impedance with respect to the bus of interest, the final formulation is obtained.

$$SCR = \frac{S_{SC}}{S_{bus}} \rightarrow \frac{V_g^2}{S_n * Z_g} \rightarrow \frac{1}{Z_{g-pu}} \tag{5}$$

Inequality constraints $\mathcal{C}_{opt}$ in (6) are formulated to allow for better behavior of the optimization algorithm, such as X/R_{min} and X/R_{max}, with values 3 and 15 respectively. X/R is the ratio between the reactance and resistance of the grid impedance. For the contraints SCR_{min} and SCR_{max} are 1.3 and 10. The values for V_{max} and V_{min} are 0.92 and 1.08 respectively. The selected optimization tolerance was $1e^{-12}$. However, other tolerances were tested and also proved to work.

$$\mathcal{C}_{opt} = \begin{cases} X_g \leq X/R_{max} * R_g \;;\; X_g \geq X/R_{min} * R_g \\ R_g^2 + X_g^2 \geq \frac{1}{SCR_{max}^2} \;;\; R_g^2 + X_g^2 \leq \frac{1}{SCR_{min}^2} \\ V_g \leq V_{max} \;;\; V_g \geq V_{min} \end{cases} \tag{6}$$

III. Verification

A. EMT Simulation

A fully validated EMT model of a type IV WTG employing actual converter control source code was used to simulate different operating conditions in a single-machine infinite-bus system (SMIB). The results with a data sampling time of 1.0 (ms) for a simulation of 140 (s) are shown in Fig. (2). WTG experiences several changes in operating points, including power and voltage reference, as well as SCR at the point of interconnection. The graph at the lowermost is the estimation of SCR using the proposed method. The values for voltage, active power, and reactive power are also plotted in the upper graphs of the figure. It shall be noted that the SCR is changed by altering the grid impedance via circuit breakers in the simulation. This forced the voltage to sink below the fault detection threshold of the WTG converter on two occasions at 100 (s) and 120 (s). This emulates a realistic scenario where drastic changes in SCR usually follow a voltage dip, as faulty sections of the system need isolation. Nonetheless, the SCR estimation remains robust and stable throughout these changes.

In the SCR graph, the green and red dotted lines represent COBYLA and SLSQP algorithms. Apart from a few areas, the two methods produced close results, although calculating differently. SLSQP was found to be 10-30 times faster than COBYLA. In order to understand the impact of the tolerance, tests were conducted for tolerances ranging from $1e^{-8}$ to $1e^{-12}$, represented by the gray area. Despite the two different algorithms and tolerances, the estimations are in line or close to expectations.

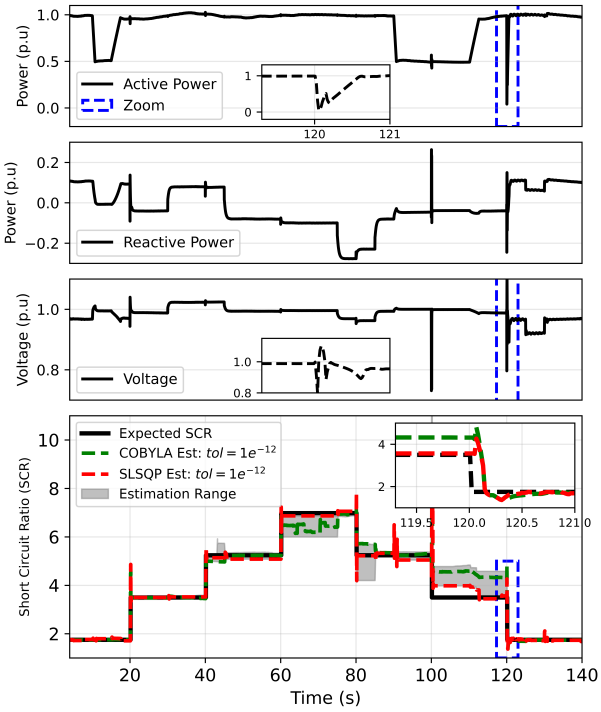

Fig. 2. SCR Estimation for EMT Simulation.

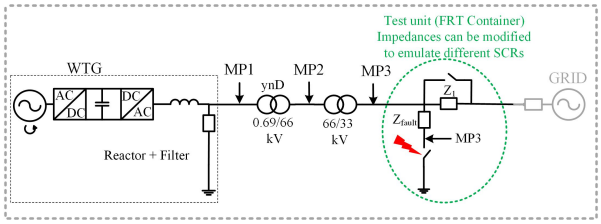

Fig. 3. Full-Scale Field WTG with FRT container to modify impedances

B. Field WTG

The field tests were conducted at a site in Østerild, Denmark, in 2023, using fault ride-through (FRT) test containers connected between the wind turbine and the grid. The impedance of the test container was adjusted by changing its internal structure with switches and reactors. The procedure involves activating a larger impedance 15 seconds before applying a fault at 60 seconds. The FRT container was configured with an impedance switch sized according to the rated power of the wind turbine, enabling accurate SCR emulation at the turbine's monitoring points. As shown in Fig. (3), the site included three measurement points (MPs). Fig. (4) displays results from one of the tests. The expected SCR values for the system in front of the wind turbine were calculated based on the best estimates of the grid and known impedances of on-site components, accounting for tolerances and non-linearities. The estimated values closely matched the expected outcomes, and the algorithm was verified with additional tests.

C. Operational Wind Power Plant

In Fig (5), the results from a test in an operational WPP are shown, with a data sampling time of 150 (ms) and

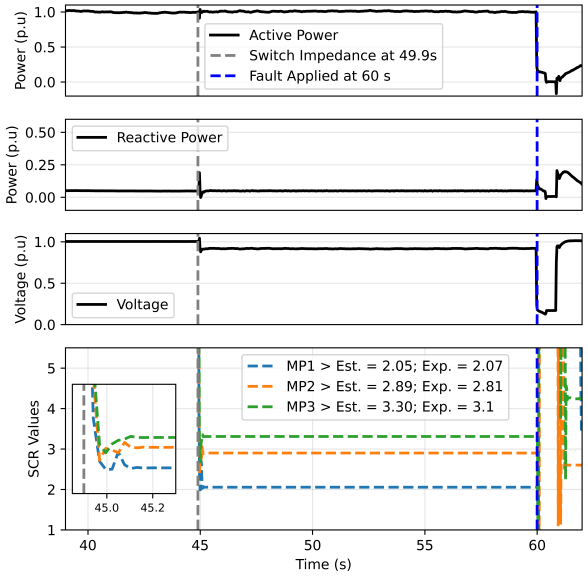

Fig. 4. Full-Scale Field WTG: SCR estimation for one case

around 20 (hrs) of measurement, where the top three graphs show active power, reactive power, and voltage respectively. During the day, these values vary continuously, but the grid impedance estimation is maintained relatively constant. The tests were carried out together with the local TSO, where a short transmission line close to the WPP is opened to alter the SCR, leaving only one long line connecting the WPP to the system. Before opening the transmission line, the WPP power was ramped down to zero. The SCR estimation stays around 7.5-8 for a few hours until the short line is opened. After opening and ramping up the power to 30 %, the SCR estimation reaches a steady state of around SCR = 2. This result is in agreement with the expectations of the local TSO.

The SCR estimation in red shows the raw SCR estimations, whereas black shows the 30-second moving average applied to the estimation. In the optimization algorithm, it is found that for high SCRs where the impedance is quite small, even very small errors in the measurement can lead to larger changes in SCR of around 20-30%. However, this region of SCR or grid impedance is generally not critical for operation. When the SCR reaches lower values, meaning grid impedances are higher, as observed in Fig. 5, the estimations tend to be more accurate as small movements of the grid impedance tend to generate more changes in voltage and power.

IV. Conclusion

A new method for equivalent grid fundamental frequency impedance estimation is presented. The method has been verified against EMT simulation and real measurements from a field WTG and an operational WPP. Controlled events were applied to force the grid impedance to change. Results show that the method is accurate for most scenarios, proving to be a reliable source of information for grid impedance estimation that can be further used both at the component and plant level. For future work, the following are suggestions for studies regarding the method. First, the possibility of applying the

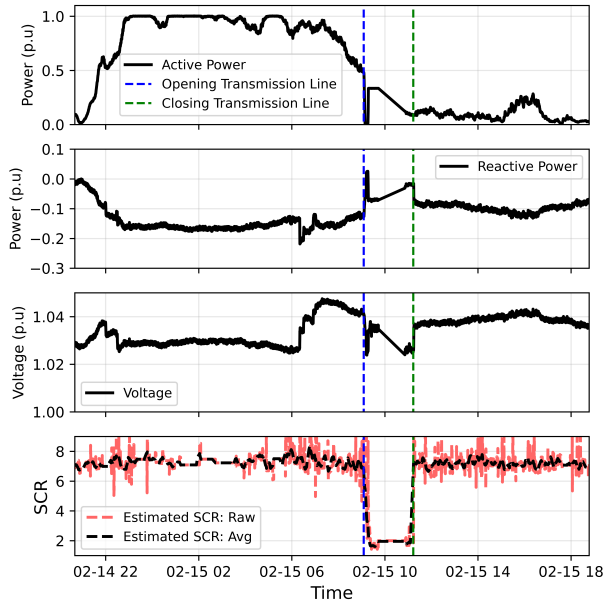

Fig. 5. Operational Wind Power Plant: SCR Estimation where the transmission line has been opened (red dotted line) to allow the SCR to drop and has been closed again (green dotted line).

method to estimating grid impedance in other frequencies shall be evaluated. Second, the speed and the reliability of the estimations can be studied depending on the use-case desired. Finally, the method should also be tested for situations where a large number of converters is present in the grid.

REFERENCES

[1] J. Matevosyan, J. MacDowell, N. Miller, B. Badrzadeh, D. Ramasubramanian, A. Isaacs, R. Quint, E. Quitmann, R. Pfeiffer, H. Urdal, T. Prevost, V. Vittal, D. Woodford, S. H. Huang, and J. O'Sullivan, "A Future With Inverter-Based Resources: Finding Strength From Traditional Weakness," *IEEE Power and Energy Magazine*, vol. 19, no. 6, pp. 18–28, 2021.

[2] S. Dutta, D. Ramasubramanian, M. Bello, W. Zhou, N. Mohammed, and B. Bahrani, "Analytical Methods for Determination of Stable Operation of IBRs in Future Power System," in *2024 IEEE Power Energy Society General Meeting (PESGM)*, 2024, pp. 1–5.

[3] M. K. De Meerendre, E. Prieto-Araujo, K. H. Ahmed, O. Gomis-Bellmunt, L. Xu, and A. Egea-Àlvarez, "Review of Local Network Impedance Estimation Techniques," *IEEE Access*, vol. 8, 2020.

[4] Y. Cheng, W. Wu, Y. Yang, E. Koutroulis, H. S.-H. Chung, M. Liserre, and F. Blaabjerg, "Zero-Sequence Voltage Injection-Based Grid Impedance Estimation Method for Three-Phase Four-Wire DC/AC Grid-Connected Inverter," *IEEE Transactions on Industrial Electronics*, pp. 1–7, 2023.

[5] D. Serfontein, J. Rens, G. Botha, and J. Desmet, "Continuous Event-Based Harmonic Impedance Assessment Using Online Measurements," *IEEE Transactions on Instrumentation and Measurement*, vol. 65, no. 10, pp. 2214–2220, 2016.

[6] N. Hoffmann and F. W. Fuchs, "Minimal Invasive Equivalent Grid Impedance Estimation in Inductive–Resistive Power Networks Using Extended Kalman Filter," *IEEE Transactions on Power Electronics*, vol. 29, no. 2, pp. 631–641, 2014.

[7] G. M. Gomes Guerreiro, R. Sharma, F. Martin, and N. Goldenbaum, "Method for Equivalent Impedance Estimation in Electrical Systems." European Patent Application No. EP24194841.3 A1, filed Aug. 16, 2024, not published.

[8] D. Kraft, "A Software Package for Sequential Quadratic Programming, 1 st Edition," *DFVLR, Cologne*, 1988.

[9] M. J. D. Powell, "Direct search optimization method that models the objective and constraint functions by linear interpolation." Dordrecht: Springer Netherlands, 1994, pp. 51–67.